Respiratory Physiology & Neurobiology 258 (2018) 5–11

Contents lists available at ScienceDirect

Respiratory Physiology & Neurobiology

journal homepage: www.elsevier.com/locate/resphysiol

A simulation study of diffusion-convection interaction and its effect on multiple breath washout indices

Sylvia Verbanck[a,*], Manuel Paiva[b]

[a] Respiratory Division, University Hospital UZ Brussel, Vrije Universiteit Brussel, Brussels, Belgium
[b] Respiratory Division, University Hospital Erasme, Université Libre de Bruxelles, Brussels, Belgium

ARTICLE INFO

Keywords:
Lung model simulations
Convective and diffusive gas transport
Acinar ventilation heterogeneity

ABSTRACT

Experimental studies of acinar ventilation heterogeneity (S_{acin}) derived from the multiple breath washout have shown the potential of S_{acin} to pick up structural change in lung disease. Recent S_{acin} data suggest that even when intra-acinar structure is unaltered, the combination of convection, diffusion and number of acini fed by patent terminal bronchioles can modify S_{acin}. We show here how S_{acin} is affected by structural features such as the secondary alveolar septa, intra-acinar ramification and number of ventilated acini. The simulations also predict relationships between respective alterations in S_{acin} and washout indices such as lung clearance index (LCI) and alveolar mixing efficiency (AME). This was verified experimentally, with highly significant correlations between S_{acin} and LCI ($r = +0.85; p < 0.001$) and between S_{acin} and AME ($r = -0.92$; $p < 0.001$). We have shown how acinar ventilation heterogeneity can be affected by a reduction of number of ventilated acini, a change in overall alveolization or in intra-acinar alveolization pattern, via their impact on the balance between convection and diffusion at acinar level.

1. Introduction

A few decades ago multiple breath washout (MBW) indices derived from normalized phase III slope analysis have been introduced in an attempt to separate convection-dependent ventilation heterogeneities from more peripherally located ventilation heterogeneities (Crawford et al., 1985). The respective mechanisms were coined convection-dependent inhomogeneities and diffusion-convection-dependent inhomogeneities. The quantification of phase III slope analysis via indices termed S_{cond} and S_{acin} was meant to provide an anatomical point of reference, given that the main site of occurrence of convection-dependent and diffusion-convection-dependent inhomogeneities is in the conductive and the acinar airways, respectively (Verbanck et al., 1997). The physiological dividing line between S_{cond} and S_{acin} is the so-called diffusion front, which arises when a test gas is inhaled and a sigmoid-like curve of test gas concentration develops between the mouth and the lung periphery. The diffusion front occurs in the zone where total airway lumen cross section shows a marked increase with generation number, i.e., where diffusive gas transport progressively takes over from convective gas transport. Under normal breathing conditions, the diffusion front is established within a fraction of a second, and only on the peripheral side of the diffusion front does concentration continue to increase as test gas is continuously being inspired; it is therefore referred to as 'quasi-static'. The first numerical simulation of the diffusion front in an anatomically realistic model of the lung periphery with identical acini (Paiva et al., 1976) indicated that S_{acin} for nitrogen was produced inside each acinus; this was later confirmed by simulations that could be based on newer anatomical data of the human acinus (Dutrieue et al., 2000). More recent model simulations in clusters of acini, but with terminal bronchioles originating in generations 14 to 17 basically confirmed that diffusion-convection interaction which causes a non-zero S_{acin}, was mainly operational beyond the terminal bronchioles (Henry et al., 2012).

We have recently shown how the complete obstruction of a considerable number of terminal bronchioles, as has been suggested to occur in COPD (McDonough et al., 2011), can affect S_{acin} (Verbanck et al., 2018). We speculated that the inspiratory flow that would normally be distributed over approximately 30.000 acini is distributed over considerably fewer acini in COPD, resulting in greater local convective velocities, affecting diffusion-convection-dependent inhomogeneity and thus S_{acin}. We suggested that the effect on S_{acin} of increased local velocity, due to flow being distributed over fewer terminal bronchioles, was akin to the single breath phaseIII slope increase observed experimentally in normal subjects breathing at higher flow rates (Paiva et al., 1988). Importantly, the S_{acin} increase in the particular case of COPD patients with negligible emphysema illustrated

* Corresponding author.
E-mail address: sylvia.verbanck@uzbrussel.be (S. Verbanck).

https://doi.org/10.1016/j.resp.2018.09.010
Received 2 August 2018; Received in revised form 11 September 2018; Accepted 25 September 2018
Available online 27 September 2018

how S_{acin} changes could arise from a model with preserved intra-acinar structure, solely due to an altered balance between convection and diffusion. These new experimental observations in smokers, and the simulation study by Henry et al. (2012) motivated the present simulation study to explore how exactly diffusion-convection interaction and intra-acinar structure can affect S_{acin}.

The main goal of this simulation study was to determine the extent to which specific pathologic changes in inter- and inter-acinar structural features can impact S_{acin}. We also examined the associated effect of such changes on the most commonly used MBW index, the lung clearance index (LCI) determined in the latter part of a MBW test, and on the alveolar mixing efficiency (AME) derived from the early part of the MBW concentration curve (Crawford et al., 1989). Finally, we verified whether the relationships between S_{acin} and LCI or AME predicted by the simulations, hold in the experimental MBW data retrieved from our recent smoker study (Verbanck et al., 2018).

2. Methods

The premise of the simulations presented here was that there be no parameter fitting. The geometry of the model was based on anatomical data (Haefeli-Bleuer and Weibel, 1988), and was only altered to illustrate the specific effect of a specific morphometric feature (such as secondary alveolar septa). Parameter fitting would have been necessary if one also wanted to simulate S_{cond}, since there are several competing mechanisms that could potentially generate a non-zero and indeed positive S_{cond} value (Wilson, 2013; Verbanck and Paiva, 2016; Foy and Kay, 2017), but no experimental verification favoring one over the other.

2.1. The reference model and two alternative model configurations

For the model geometry, we used a 14-acinar-cluster arrangement proposed by Henry et al (2012) but in one instead of two lung zones, since our study focusses on peripheral ventilation heterogeneity. The acini started in generations 14 to 17 and 1964 such clusters constituted an entire lung with 27,500 acini. Since the acinar cluster started in bronchial generation 11, we added 120 ml dead space (divided by 1964 clusters) to account for mouth cavity and the volume of trachea and generation 1–10 airways. For the intra-acinar airway geometry, we used either the realistic multi-branch-point model from Dutrieue et al (2000) or its trumpet model equivalent (which corresponds to a perfectly symmetrically branching acinus, where all identic parallel intra-acinar airways are lumped). This resulted in the 3 model configurations illustrated in Fig. 1A : “14-realistic-acini” (where intra-acinar ducts have secondary alveolar septa), and “14-symmetric-acini”, where intra-acinar ducts are considered with or without secondary alveolar septa. The gas transport equations were those described in Dutrieue et al (2000), where inspired test gas concentration (pure O_2) is considered constant at the entrance of each acinar cluster throughout each inspiration after dead space (120 ml) has been (re)inspired. Throughout the breathing cycle, a reflection boundary condition was situated at each acinar end. Oxygen-nitrogen binary diffusion coefficient was set to 0.225 cm^2/s.

2.2. Effect of intra-acinar structural features

When simulations interrogated the specific effect of the secondary alveolar septa on S_{acin}, the inner and outer diameters (d_{in}, d_{out}) of the alveolated intra-acinar airways as provided by Haefeli-Bleuer and Weibel (1988) were both set to the d_{out} value. In this case, effective axial diffusion was artificially increased since axial diffusion for the entire alveolated duct is no longer delayed by the alveolar septa according to the relationship $D.(d_{in}^2/ d_{out}^2)$ (Verbanck and Paiva, 1988); the ratio d_{in}^2/ d_{out}^2 typically has a value ranging 0.2–0.3 in the fully alveolated ducts, consistent with MRI measurements of apparent

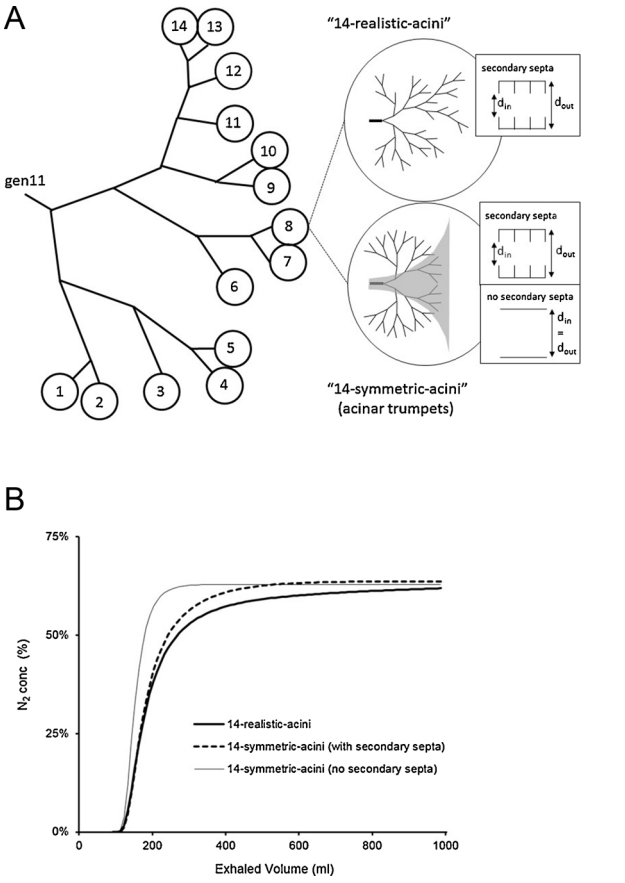

Fig. 1. Panel A: Three basic model configurations. In the “14-realistic-acini” configuration, each of the 14 acini consists of a realistic asymmetric branching pattern, with each alveolated duct characterized by secondary alveolar septa. In both “14-symmetric-acini” configurations (either with or without secondary alveolar septa), each of the 14 acini consists of a symmetric branching pattern, which corresponds to an acinar trumpet (since all parallel intra-acinar airways can be lumped). Panel B: Expired N_2 concentration curves as a function of exhaled volume following a simulation of a 1 L O_2 inspiration from a 3 L lung with initial N_2 concentration set at 80%. Solid line: “14-realistic-acini” configuration; dashed line: “14-symmetric-acini” configuration with preserved secondary alveolar septa; thin solid line: “14-symmetric-acini” configuration without secondary alveolar septa.

diffusion coefficient in the alveolar zone (Sukstanskii and Yablonskiy, 2008). In the absence of any morphometric data on arrangement of intra-acinar airspace enlargement in disease, the effect of an altered pattern in intra-acinar alveolization was simply illustrated by considering $d_{in} = d_{out}$ in selected places according to 2 simple patterns. In one intra-acinar alveolization pattern, d_{in} was set to d_{out} in subsequent intra-acinar generations, along the pathway following the shortest unit at each subsequent intra-acinar bifurcation through to the acinar end. In the other intra-acinar alveolization pattern, this was done along the pathway following the longest units through to the acinar end.

2.3. Effect of number of acini and acinar expansion

When simulations required the reduction of the number of terminal bronchioles, for instance by a factor 2, only half the number of 14-acinar clusters (982 instead of 1964) were considered to make up the entire lung. This implied that the total breathing flow was distributed over only half of the normal number of acini, hence convective flow at the level of the terminal bronchioles became double compared to the reference configuration. When simulations interrogated the effect of heterogeneity in specific ventilation of the acini, this was done by